# An X-Ray Diffraction Study on the Structures of Monochloropentakis(*N,N*-dimethylformamide)copper(II), Trichloromono(*N,N*-dimethylformamide)- and Tetrachlorocuprate(II) Complexes in *N,N*-Dimethylformamide

Kazuhiko Ozutsumi, Shin-ichi Ishiguro,* and Hitoshi Ohtaki†
Coordination Chemistry Laboratories, Institute for Molecular Science, Myodaiji, Okazaki 444
†Department of Electronic Chemistry, Tokyo Institute of Technology, Nagatsuta-cho 4259, Midori-ku, Yokohama 227
(Received August 17, 1987)

The structure of the monochlorocopper(II), trichloro- and tetrachlorocuprate(II) complexes in *N,N*-dimethylformamide (DMF) has been studied by the X-ray diffraction method at 25 °C. The radial distribution curve obtained for a solution containing the monochlorocopper(II) complex as the predominant species reveals the presence of an axially elongated octahedral $[CuCl(dmf)_5]^+$ complex, three Cu–O(eq) and two Cu–O(ax) bond lengths being 199(1) and 239(4) pm, respectively. The chloride ion binds to the copper(II) ion at the equatorial site and the Cu–Cl distance is 220(2) pm. The Cu–O(eq) bond length within the $[CuCl(dmf)_5]^+$ complex is practically the same as that within the $[Cu(dmf)_6]^{2+}$ (203 pm). The X-ray scattering data of solutions containing the tri- and tetrachlorocuprate(II) complexes as the main species are well explained in terms of the existence of the distorted tetrahedral $[CuCl_3(dmf)]^-$ and $[CuCl_4]^{2-}$ complexes, respectively, in the solutions. The Cu–Cl and Cu–O bond lengths within the $[CuCl_3(dmf)]^-$ complex are 219(1) and 230(13) pm, respectively. The Cu–O distance within the complex is longer than that of the equatorial Cu–O bond within the $[Cu(dmf)_6]^{2+}$ and $[CuCl(dmf)_5]^+$ ions. The Cu–Cl bond length within the $[CuCl_4]^{2-}$ complex is 226(1) pm and is longer than that within the $[CuCl_3(dmf)]^{2-}$ complex. The nonbonding Cl···Cl distances within the $[CuCl_4]^{2-}$ complex are 346(3) and 412(6) pm.

The structure of complexes between copper(II) and chloride ions in aqueous $CuCl_2$ solutions with varying concentrations has been investigated by X-ray,[1,2] neutron diffraction,[3] and EXAFS methods,[4] and the data are interpreted in terms of the formation of various monomeric and/or polymeric chloro complexes. X-Ray scattering measurements have also been carried out for methanolic solutions of $CuCl_2$ and the presence of monomeric complexes with various numbers of chloride ions was proposed in the solutions.[5] However, the data analysis of the solutions so far examined was performed for the average structure of some complexes coexisting and no structural information has been given for individual complex species in solution with adjusting the concentration ratios of copper(II) to chloride ions on the basis of the stability constants of copper(II)–chloro complexes.

The structure of the $[CuCl_3]^-$ and $[CuCl_4]^{2-}$ complexes in crystal has been investigated from magnetic and thermochromic points of view. The former complex has been concluded to have a dimeric structure with a square-planar coordination geometry around a copper(II) ion,[6–8] and the latter has either a square-planar or a distorted tetrahedral structure.[9–18] The structure of the complexes in solution, however, has never been studied.

A series of mononuclear copper(II)–chloro complexes are formed and formation of the complexes is enhanced in aprotic solvents such as *N,N*-dimethylformamide (DMF), dimethyl sulfoxide, and acetonitrile and the formation constants of each complex have been determined.[19–22] In DMF the mono-, tri-, and tetrachloro complexes of copper(II) ion are formed as the main species at suitable concentration ratios of chloride to copper(II) ions.[19] Therefore, in the present study we determined the structure of the monochlorocopper(II), trichloro- and tetrachlorocuprate(II) complexes in DMF by the X-ray diffraction method. The structure of the dichlorocopper(II) complex was not determinable because the formation of the complex is suppressed in DMF.

## Experimental

**Preparation of Sample Solutions.** All chemicals used were of reagent grade. *Copper(II) perchlorate DMF solvate* was prepared by the method described in a previous paper.[19] *Copper(II) chloride* was prepared by dissolving copper(II) oxide in hydrochloric acid and then recrystallized from aqueous dilute hydrochloric acid and dried in a vacuum oven at 100 °C. *Lithium chloride* was recrystallized from water and dried in vacuum at 200 °C. *N,N*-Dimethylformamide was purified as described elsewhere.[19]

Sample solutions A to D were prepared as listed in Table 1. Solution A was prepared by dissolving anhydrous

Table 1. The Composition (mol dm$^{-3}$), Stoichiometric Volumes $V$ per Copper Atom and Densities $\rho$ of the Sample Solutions

| | A | B | C | D |
|---|---|---|---|---|
| $Cu^{2+}$ | 1.189 | 1.380 | 1.358 | 1.081 |
| $Cl^-$ | 1.202 | 4.178 | 5.351 | 4.685 |
| $Li^+$ | — | 1.418 | 2.635 | 2.523 |
| $ClO_4^-$ | 1.176 | — | — | — |
| DMF | 12.28 | 12.06 | 11.87 | 12.10 |
| $V/10^9$ pm$^3$ | 1.397 | 1.203 | 1.223 | 1.536 |
| $\rho$/g cm$^{-3}$ | 1.133 | 1.127 | 1.162 | 1.137 |
| $C_{Cl}/C_{Cu}$ | 1.011 | 3.027 | 3.940 | 4.334 |

copper(II) chloride and copper(II) perchlorate DMF solvate in DMF and solutions B to D by dissolving anhydrous copper(II) and lithium chlorides. Mole ratios $C_{Cl}/C_{Cu}$, where $C_i$ represents the total concentration of species $i$, were so chosen that solutions A, B, and C contained the mono-, tri-, and tetrachloro complexes, respectively, as the main species according to the formation constants in the literature.[19] Since the solubility of LiCl in DMF is not sufficiently large, the tetrachlorocuprate(II) complex is not fully yielded in DMF. The yield of the complex in solution C was about 70 mol% of the total copper(II) ions, and therefore, in order to check the reproducibility of the structural analysis, solution D with the slightly higher $C_{Cl}/C_{Cu}$ mole ratio than that of solution C was also examined. Solution A thus prepared is green, solution B orange and solutions C and D yellow. Concentrations of copper(II) ions in the sample solutions were determined by electrogravimetry. Concentrations of chloride ions were gravimetrically determined as AgCl. Concentrations of perchlorate ions in solution A and lithium ions in solutions B to D were evaluated by the material balance of ions in the solutions. Densities of the test solutions were measured pycnometrically.

**X-Ray Scattering Measurements.** X-Ray scattering measurements were performed on a $\theta$–$\theta$ type diffractometer (JEOL DX-GO-Y) by using Mo $K\alpha$ radiation ($\lambda$=71.07 pm). The method of measurements and data treatments are described elsewhere.[23] The accessible range of scattering angle ($2\theta$) was 2—140°, which corresponds to the scattering vector ($s=4\pi\lambda^{-1}\sin\theta$) range of $0.3\times10^{-2}$—$16.6\times10^{-2}$ pm$^{-1}$. Times required to accumulate 160000 counts were recorded at each angle of $2\theta$.

The reduced intensities $i(s)$ were extracted from the measured intensities $I(s)$, which had been scaled to the absolute ones after corrections for absorption, polarization and double scatterings of X-rays, according to Eq. 1:

$$i(s) = I(s) - \sum_i n_i[\{f_i(s) + \Delta f_i'\}^2 + (\Delta f_i'')^2], \quad (1)$$

where $n_i$ is the number of atom $i$ in a stoichiometric volume $V$ per copper atom and $f_i(s)$ denotes the atomic scattering factors at $s$ of atom $i$. $\Delta f_i'$ and $\Delta f_i''$ represent the real and imaginary parts of anomalous dispersion, respectively. The reduced intensities multiplied by $s$ of the sample solutions are depicted in Fig. 1. The $s\cdot i(s)$ values were converted by the Fourier transform into the radial distribution function $D(r)$ as

$$D(r) = 4\pi r^2\rho_o + \frac{2r}{\pi}\int_0^{s_{max}} s\cdot i(s)\cdot M(s)\cdot\sin(rs)ds, \quad (2)$$

where $\rho_o$ is the average scattering density in a stoichiometric volume of the solution and $s_{max}$ denotes the maximum $s$-value attained in the measurement. $M(s)$ is the modification function defined as

$$M(s) = \frac{\sum_i n_i\{(f_i(0) + \Delta f_i')^2 + (\Delta f_i'')^2\}}{\sum_i n_i\{(f_i(s) + \Delta f_i')^2 + (\Delta f_i'')^2\}}\cdot\exp(-ks^2) \quad (3)$$

The damping factor $k$ was chosen as 100 pm$^2$ in the present study. The differential radial distribution curves, $D(r)-4\pi r^2\rho_o$, for solutions A to D are shown in Fig. 2.

All calculations were performed by using programs KURVLR[24] and NLPLSQ.[25]

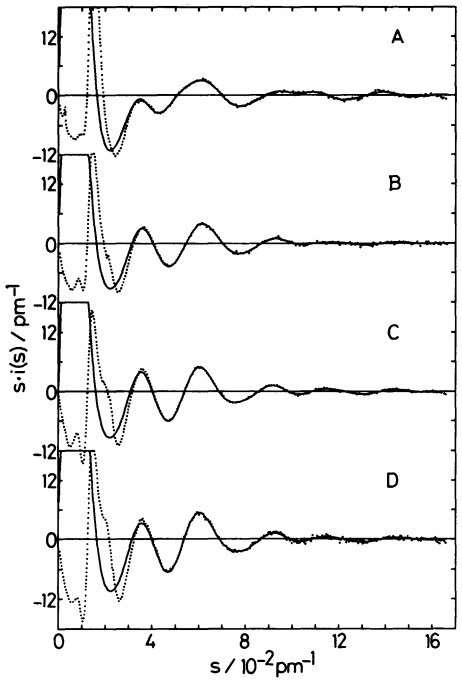


Fig. 1. The reduced intensities multiplied by $s$ for solutions A, B, C, and D. The observed $s\cdot i(s)$ values are shown by the dotted lines and calulated ones by the solid lines.

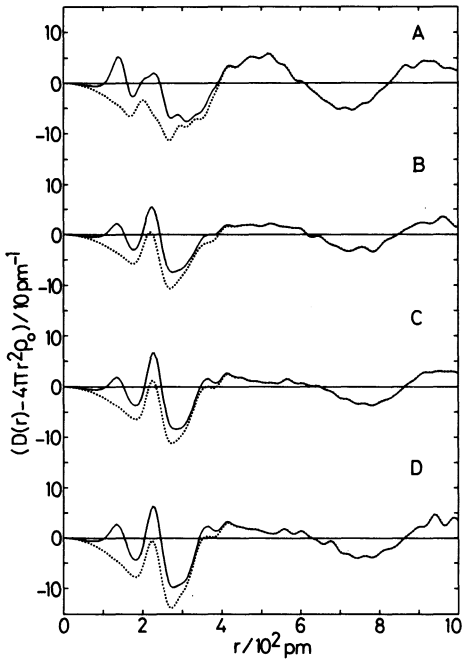


Fig. 2. The differential radial distribution curve, $(D(r)-4\pi r^2\rho_o)$, for solutions A, B, C, and D (solid lines). The dotted lines represent the residual curves after subtracting peaks due to the intramolecular interactions of DMF molecules for solutions A to D and perchlorate ions for solution A.

## Results and Discussion

**Structure of the $[CuCl]^+$ Complex.** According to the stability constants for the copper(II)-chloro complexes in DMF,[19] the $[CuCl]^+$ complex is expected to be formed as the predominant species in solution A. Figure 3 depicts the $(D(r)-4\pi r^2\rho_o)$ curve of solution A as well as the calculated peak shapes for atom pairs in the solution which will be discussed later. In the curve four peaks appear around 130, 230, 290, and 410 pm, and a shoulder and a small hump are also observed at about 200 and 320 pm, respectively.

From the X-ray analysis of liquid DMF[26] it was shown that two peaks originating from the intramolecular interactions within DMF molecule appeared at 130 and 230 pm in the radial distribution function and no appreciable intermolecular interactions are observed because of its disordered liquid structure. Accordingly, the first peak at 130 pm should be due to the C-H, C=O, and C-N bonds within DMF molecules. The Cl-O bonds within perchlorate ions are also contained in the peak. The second peak at about 230 pm with a shoulder at 200 pm may be ascribable to interactions between copper(II) ion and ligand atoms within the monochlorocopper(II) complex. The nonbonding N···O, C···C, and C···O interactions within DMF molecules and the O···O contacts within perchlorate ions also contribute to the peak. The third peak and a small hump at 290 and 320 pm, respectively, may be due to the Cu···C interactions and the nonbonding interligand interactions within the monochlorocopper(II) complex. The Cu···N(DMF) nonbonding interactions should be involved in the peak at 410 pm as have been seen in the solvated copper(II) ion.[27]

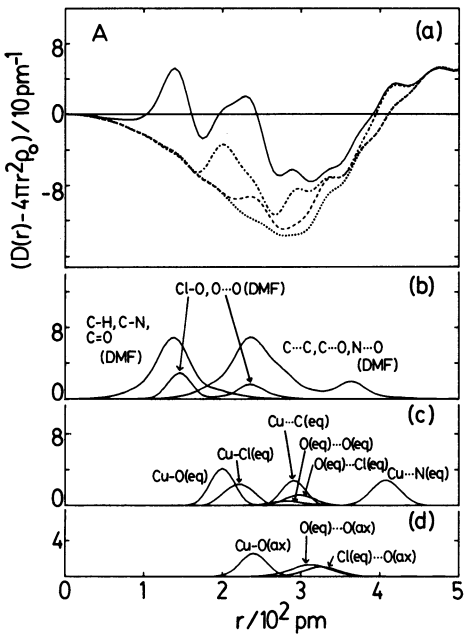


Fig. 3. (a) The $(D(r)-4\pi r^2\rho_o)$ curve for solution A. (b) The theoretical peaks for intramolecular interactions within DMF molecule and perchlorate ion. (c) The theoretical peak shapes due to the Cu-O(eq), Cu-Cl(eq), Cl···Cl, Cl···O, Cu···C(eq), and Cu···N(eq) interactions within the monochloropentakis(*N*,*N*-dimethylformamide)copper(II) complex. (d) The calculated peaks for Cu-O(ax), Cl···Cl, and Cl···O interactions within the mono-complex. The chain, dashed and dotted lines represent the residual curves after subtraction of the theoretical peaks in (b), (c), and (d), respectively.

At the first step of analysis of the radial distribution curve, the theoretical peak shapes due to the intramolecular interactions within DMF molecules and perchlorate ions were subtracted from the original curve. The structural parameter values were assumed to be the same as those obtained in liquid DMF and are quoted from the literature.[26] The residual curve drawn by the chain line (Fig. 3a) shows a large peak at 200 pm with a shoulder at 230 pm and three peaks around 290, 320, and 400 pm, which are all ascribable to the intramolecular interactions within the $[CuCl]^+$ complex. The peak at 200—230 pm should be due to the bonds between copper(II) ion and ligand atoms within the complex and the peak shape suggests that it consists of at least two interactions. However, the peak shape could not be analyzed by any assumption of only two kind Cu-O (ca. 200 pm) and Cu-Cl (ca. 230 pm) bonds with the values of the temperature factor of 20 and 70 $pm^2$,[3,5] respectively, and was possible to be explained by the introduction of a distorted octahedral model of the monochlorocopper(II) complex with three kinds of bonds: i.e., the equatorial Cu-O bond (ca. 200 pm) with the frequency factor 3, an equatorial Cu-Cl (ca. 220 pm) and two axial Cu-O bonds (ca. 240 pm). Moreover, the small peak observed at 320 pm was also explainable from the distorted octahedral model to be nonbonding interligand Cl(eq)···O(ax) interactions. The radial distribution curve and reduced intensities calculated on the basis of other structure models such as a square-planar four-coordination, a trigonal bipyramidal or a square pyramidal five-coordination structure did not fit the experimental values. Therefore, the monochlorocopper(II) complex was concluded to have a distorted octahedral structure.

The structure parameters of the $[CuCl(dmf)_5]^+$ complex were refined by a least-squares calculation for the $s\cdot i(s)$ curve over the region $s>4\times10^{-2}$ $pm^{-1}$, where the intramolecular interactions within the complex and those of DMF molecules and perchlorate ions mainly contribute to the $s\cdot i(s)$ values. In order to avoid errors introduced by neglecting long-range intermolecular interactions, the lower limit of the $s$-values was varied from $4\times10^{-2}$ to $7\times10^{-2}$ $pm^{-1}$. In the course of the calculation, the parameter values for the intramolecular interactions of DMF and perchlorate ion were fixed at the literature values.[26,28]

Table 2. Results of the Least-Squares Refinements of Solution A. Standard Deviations Are Given in Parentheses

| Interaction | Parameter | A-I ($s>4\times10^{-2}$ pm$^{-1}$) | A-II ($s>5\times10^{-2}$ pm$^{-1}$) |
|---|---|---|---|
| Cu–O(eq) | $r$/pm | 199(1) | 199(1) |
| | $b$/10 pm$^2$ | 1(1) | 1(1) |
| | $n$ | 3[a] | 3[a] |
| Cu–Cl(eq) | $r$/pm | 220(2) | 221(3) |
| | $b$/10 pm$^2$ | 12(4) | 14(5) |
| | $n$ | 1[a] | 1[a] |
| Cu–O(ax) | $r$/pm | 239(4) | 240(4) |
| | $b$/10 pm$^2$ | 4(1) | 3(1) |
| | $n$ | 2[a] | 2[a] |
| O(eq)···O(eq) | $r$[b]/pm | 281 | 281 |
| | $b$/10 pm$^2$ | 6[a] | 6[a] |
| | $n$ | 2[a] | 2[a] |
| Cl(eq)···O(eq) | $r$[c]/pm | 297 | 297 |
| | $b$/10 pm$^2$ | 6[a] | 6[a] |
| | $n$ | 2[a] | 2[a] |
| O(eq)···O(ax) | $r$[d]/pm | 311 | 312 |
| | $b$/10 pm$^2$ | 12[a] | 12[a] |
| | $n$ | 6[a] | 6[a] |
| Cl(eq)···O(ax) | $r$[e]/pm | 325 | 326 |
| | $b$/10 pm$^2$ | 12[a] | 12[a] |
| | $n$ | 2[a] | 2[a] |
| Cu···C(eq) | $r$/pm | 288(2) | 288(1) |
| | $b$/10 pm$^2$ | 7(2) | 5(3) |
| | $n$ | 3[a] | 3[a] |
| Cu···N(eq) | $r$/pm | 404(3) | 412(2) |
| | $b$/10 pm$^2$ | 10(4) | 7(3) |
| | $n$ | 3[a] | 3[a] |

a) The values were kept constant during the calculation. b) $r_{O(eq)\cdots O(eq)}=\sqrt{2}\,r_{Cu-O(eq)}$. c) $r_{Cl(eq)\cdots O(eq)}=\sqrt{r_{Cu-O(eq)}^2+r_{Cu-Cl(eq)}^2}$. d) $r_{O(eq)\cdots O(ax)}=\sqrt{r_{Cu-O(eq)}^2+r_{Cu-O(ax)}^2}$. e) $r_{Cl(eq)\cdots O(ax)}=\sqrt{r_{Cu-Cl(eq)}^2+r_{Cu-O(ax)}^2}$.

Some constraints were set for the distances of nonbonding interligand interactions as indicated at the footnote in Table 2 and the frequency factors of all interactions in the table were kept constant at the given values estimated from the distorted octahedral model of the complex in the course of the calculation. The Cu–O(eq), Cu–Cl(eq), and Cu–O(ax) bond distances were finally determined to be 199, 220, and 239 pm, respectively.

**Structure of the $[CuCl_3]^-$ Complex.** Solution B contains the trichlorocuprate(II) complex as the main species. Figure 4a shows the $(D(r)-4\pi r^2\rho_o)$ curve (solid line) of the solution, in which four peaks are observed around 130, 225, 360, and 410 pm. The first peak at 130 pm is due to the C–H, C=O, and C–N bonds within DMF molecules. The large peak at 225 pm is expected to be due to the Cu–Cl bonds from the sum of their ionic radii and partly to the Cu–O bonds within the $[CuCl_3]^-$ complex if some solvent molecules coordinate to copper(II) ion. The peak might also contain peaks due to intramolecular nonbonding N···O, C···C, and C···O interactions of DMF. The Li–O contacts within the solvated lithium ions also contribute, in part, to the peak as have been shown by a study of solution X-ray diffraction of solvated lithium ions.[29] However, because of the low concentration of lithium ions in solution B and the

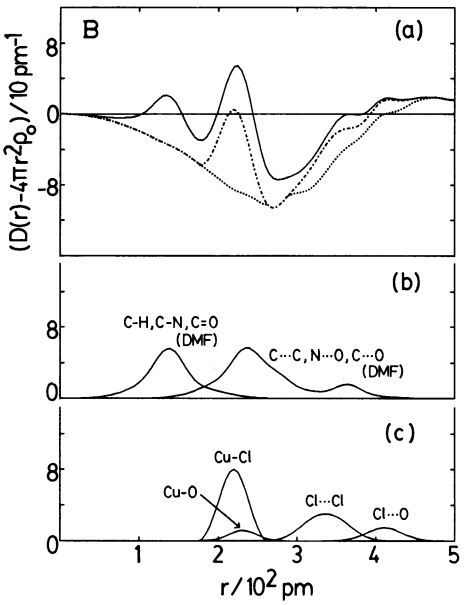


Fig. 4. (a) The $(D(r)-4\pi r^2\rho_o)$ curve for solution B, (b) The theoretical peaks for intramolecular interactions within DMF molecule. (c) The theoretical peak shapes due to the Cu–Cl, Cu–O, Cl···Cl, and Cl···O interactions within the trichloromono(*N*,*N*-dimethylformamide)cuprate(II) complex. The chain and dotted lines represent the residual curves after subtraction of the theoretical peaks in (b) and (c), respectively.

weak scattering power of lithium atom, the contribution of the solvated lithium ions to the scattered intensities is not significant, and it was neglected in the course of the data analysis. The third and fourth peaks around 360 and 410 pm, respectively, could be ascribed to the interligand interactions within the $[CuCl_3]^-$ complex.

After subtracting the theoretical peak shapes due to the intramolecular interactions within DMF molecules from the original curve, the residual curve expressed by the chain line (Fig. 4a) shows the predominant peak centered at 220 pm which can be attributed to the bonds between copper and ligand atoms in the trichlorocuprate(II) complex. The structure parameters of the complex were evaluated from the shape of the peak at 220 pm by a trial-and-error method. From the analysis a possibility of a dimeric structure ($[Cu_2Cl_6]^{2-}$) of the complex found in crystals[6-8] was ruled out since the peak area is appreciably smaller than that corresponding to four Cu–Cl bonds. The peak is well-reproduced by assuming three Cu–Cl bonds and one Cu–O bond with the lengths of 220 and 230 pm, respectively, as seen in Fig. 4a (dotted line). The Cu–O distance is also reasonably expected from the interligand interactions as discussed in the following section. The calculated $s \cdot i(s)$ values based on the structural model of $[CuCl_3(dmf)]^-$ give a better fit to the experimental ones than those of the trianglar or pyramidal $[CuCl_3]^-$ structure without a DMF molecule and of the $[Cu_2Cl_6]^{2-}$ dimer structure over $s>6\times10^{-2}$ pm$^{-1}$, where the intramolecular interactions within the complex and those of DMF molecules mainly contribute to the $s \cdot i(s)$ curve.

In the residual curve (chain line in Fig. 4a) two peaks, besides the peak at 220 pm, appear at about 350 and 410 pm which may be attributable to various combinations of nonbonding Cl···Cl and Cl···O interactions within the $[CuCl_3(dmf)]^-$ complex. These peaks could not be originated from a square-planar structure with the Cu–Cl bond length of 220 pm. The two peaks at 350 and 410 pm are only explainable when the complex has a distorted tetrahedral structure with the Cu–Cl and Cu–O bond distance of 220 and 230 pm, respectively.

A least-squares method was applied to the high-angle region ($s>4\times10^{-2}$ pm$^{-1}$) of the $s \cdot i(s)$ curve in order to refine the structural parameters obtained for the $[CuCl_3(dmf)]^-$ complex by a trial-and-error method. The initial structure parameter values inserted were those estimated from the analysis of the radial distribution curve as mentioned previously. In the course of the calculation the frequency factors of each interatomic interaction were kept at the same values as those obtained from the distorted tetrahedral model of the complex. The results are summarized in Table 3. The Cu–Cl and Cu–O lengths are finally evaluated to be 219 and 230 pm, respectively.

**Structure of the $[CuCl_4]^{2-}$ Complex.** The radial distribution curves for solutions C and D illustrated in Figs. 5 and 6, respectively, were analyzed by essentially the same procedure as that employed for solution B. Since the analysis of the intensity data by assuming the sole $[CuCl_4]^{2-}$ complex as the predominant species gave slightly different results between solutions C and D for the structure parameters of the complex, we can not neglect the $[CuCl_3(dmf)]^-$ complex coexisting in the solutions. The concentrations of the $[CuCl_3(dmf)]^-$ complex in solutions C and D are estimated to be 30 and 20 mol%, respectively, from the stability constants reported for the 1 mol dm$^{-3}$ $LiClO_4$ DMF solution.[19]

Subtraction of theoretical peaks due to the C–H, C=O, C–N, N···O, C···C, and C···O interactions within DMF molecules and the Cu–Cl, Cu–O, Cl···Cl, and Cl···O pairs within the $[CuCl_3(dmf)]^-$ complex (Figs. 5b and 6b) from the radial distribution curve experimentally obtained leads to a residual curve

Table 3. Results of the Least-Squares Refinements of Solution B. Standard Deviations Are Given in Parentheses

| Interaction | Parameter | B-I ($s>4\times10^{-2}$ pm$^{-1}$) | B-II ($s>5\times10^{-2}$ pm$^{-1}$) |
|---|---|---|---|
| Cu–Cl | $r$/pm | 218(1) | 219(1) |
| | $b$/10 pm$^2$ | 8(1) | 8(1) |
| | $n$ | 3[b] | 3[b] |
| Cu–O | $r$/pm | 230(12) | 230(13) |
| | $b$[a]/10 pm$^2$ | 4[b] | 4[b] |
| | $n$ | 1[b] | 1[b] |
| Cl···Cl / Cl···O[c] | $r$/pm | 340(3) | 346(2) |
| | $b$/10 pm$^2$ | 17(2) | 18(3) |
| | $n$ | 2[b] | 2[b] |
| Cl···Cl / Cl···O[c] | $r$/pm | 410(3) | 409(4) |
| | $b$/10 pm$^2$ | 30(4) | 30(4) |
| | $n$ | 1[b] | 1[b] |

a) The values of the temperature factor were changed from 3 to 7, but practically the same results were obtained. b) The values were kept constant during the calculation. c) Assumed that $r_{Cl\cdots Cl}=r_{Cl\cdots O}$ and $b_{Cl\cdots Cl}=b_{Cl\cdots O}$.

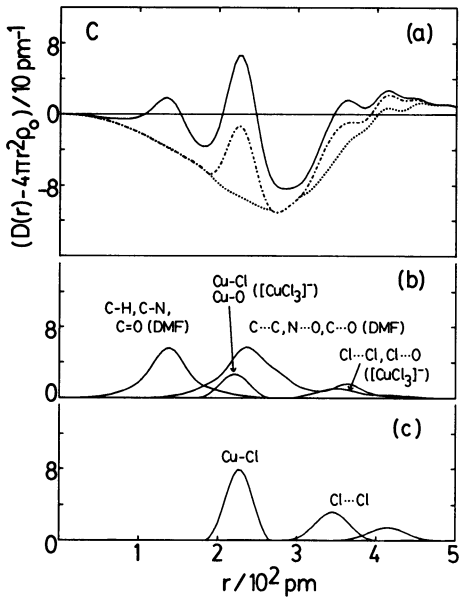


Fig. 5. (a) The $(D(r)-4\pi r^2\rho_o)$ curve for solution C. (b) The theoretical peaks for intramolecular interactions within DMF molecule and Cu–Cl, Cu–O, Cl···Cl, and Cl···O pairs within the trichloromono(*N*,*N*-dimethylformamide)cuprate(II) complex. (c) The theoretical peak shapes calculated for the Cu–Cl and Cl···Cl interactions within the tetrachlorocuprate(II) complex. The chain and dotted lines indicate the residual curves after subtracting the theoretical peaks in (b) and (c), respectively.

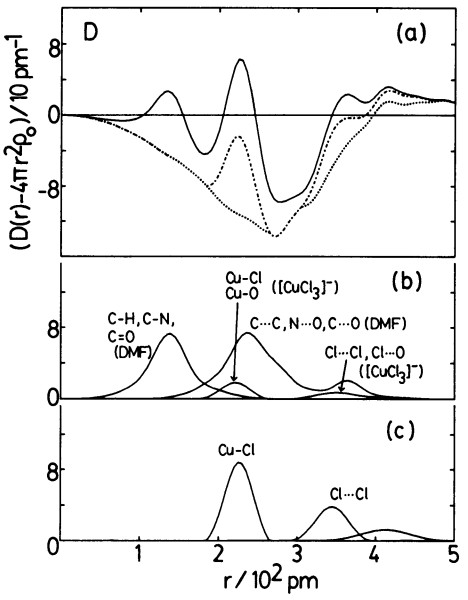


Fig. 6. (a) The $(D(r)-4\pi r^2\rho_o)$ curve for solution D. (b) The theoretical peaks for intramolecular interactions within DMF molecule and Cu–Cl, Cu–O, Cl···Cl, and Cl···O pairs within the trichloromono(*N*,*N*-dimethylformamide)cuprate(II) complex. (c) The theoretical peak shapes calculated for the Cu–Cl and Cl···Cl interactions within the tetrachlorocuprate(II) complex. The chain and dotted lines indicate the residual curves after subtracting the theoretical peaks in (b) and (c), respeactively.

Table 4. Crystal Data of the $[CuCl_4]^{2-}$ Complex Ion with Various Cations[a)]

| Complex | Distance($r$/pm) $r_{Cu-Cl}$ | $r_{Cl\cdots Cl}$ | Angle(degree) ∠Cl-Cu-Cl | Ref. |
|---|---|---|---|---|
| Square planar ($D_{4h}$) | | | | |
| $(NH_4)_2[CuCl_4]$ | 232 | 328 | 90 | 9 |
| | | 463 | 180 | |
| $(C_2H_5NH_3)_2[CuCl_4]$ | 228 | 323 | 90 | 10 |
| | | 456 | 180 | |
| $(C_3H_7NH_3)_2[CuCl_4]$ | 229 | 324 | 90 | 11 |
| | | 458 | 180 | |
| $[(NH_3CH_2CH_2)_2NH_2]Cl[CuCl_4]$ | 227 | 321 | 90 | 12 |
| | | 456 | 180 | |
| $[(C_6H_5)CH_2CH_2NH_2(CH_3)]_2[CuCl_4]$ (low temp phase) | 226 | 320 | 90 | 13 |
| | | 453 | 180 | |
| Distorted tetrahedral ($D_{2d}$) | | | | |
| $Cs_2[CuCl_4]$ | 220 | 343 | 103 | 14 |
| | | 389 | 124 | |
| $[C_6H_5CH_2N(CH_3)_3]_2[CuCl_4]$ | 226 | 344 | 99 | 15 |
| | | 413 | 133 | |
| $(CH_3NC_5H_4C_5H_4NCH_3)[CuCl_4]$ | 225 | 346 | 101 | 16 |
| | | 406 | 129 | |
| $(C_{13}H_{19}N_2OS)_2[CuCl_4]$ | 224 | 332 | 96 | 17 |
| | | 425 | 143 | |
| $[(CH_3)_3NH]_2[CuCl_4]$ | 224 | 339 | 98 | 18 |
| | | 414 | 135 | |
| $[(C_6H_5)CH_2CH_2NH_2(CH_3)]_2[CuCl_4]$ (high temp phase) | 221 | 338 | 100 | 13 |
| | | 400 | 131 | |

a) The interatomic distances and bond angles are averaged values.

(chain line in Figs. 5a and 6a), in which a major peak and two humps appear at 225, 350, and 410 pm. The peak at 225 pm is ascribable to the Cu-Cl bonds within the $[CuCl_4]^{2-}$ complex. The peak area corresponds to four Cu-Cl interactions and was found no evidence that any solvent molecule coordinated to copper(II) ion. The two humps at 350 and 410 pm, which are attributable to the nonbonding Cl···Cl interactions within the $[CuCl_4]^{2-}$ complex suggest that the complex has not a regular tetrahedral structure which should give only one peak originating from six Cl···Cl pairs at about 370 ($=225\times\sqrt{8/3}$) pm.

The structure of the $[CuCl_4]^{2-}$ complexes with various cations in crystal[9-18] can be classified into two groups; complexes in the first group are those having a square-planar structure ($D_{4h}$ symmetry) and the others have a flattened tetrahedral structure ($D_{2d}$ symmetry). Crystallographic data of these complexes are summarized in Table 4. In the square-planar complexes the Cu-Cl bond length is 226—232 pm, which is slightly longer than the Cu-Cl bond within the distorted tetrahedral complexes ($r_{Cu\text{-}Cl}$=220—226 pm). The nonbonding Cl···Cl distances within the square-planar complexes are in the range of 320—330 pm for four Cl···Cl interactions and 450—460 pm for the other two Cl···Cl interactions, while the distorted tetrahedral complexes have slightly longer Cl···Cl interactions for four Cl···Cl pairs (330—350 pm) but shorter Cl···Cl ones for the other two (400—420 pm). Since two humps are observed at 350 and 410 pm for solutions C and D (Figs. 5a and 6a, respectively), we conclude that the $[CuCl_4]^{2-}$ complex has a distorted tetrahedral structure with $D_{2d}$ symmetry.

The structure parameters for the $[CuCl_4]^{2-}$ complex were finally determined by a least-squares calculation for the $s\cdot i(s)$ values over the range $s>4\times10^{-2}$ pm$^{-1}$. The refinement was carried out by floating the values of interatomic distances and temperature factors of the complex as independent variables, while the frequency factors of the interactions were kept unchanged. The results obtained for solutions C and D are summarized in Table 5. Essentially the same results were obtained for both solutions. The Cu-Cl bond length thus determined is 226 pm and the nonbonding Cl···Cl distances are 346 and 412 pm. The Cl-Cu-Cl bond angles are 100° and 131° in the complex.

The structure of the $[CuCl(dmf)_5]^+$ complex is distorted octahedral as the $[Cu(dmf)_6]^{2+}$ ion is. The Cu-O(eq) bond length (199(1) pm) within the $[CuCl(dmf)_5]^+$ is practically the same as that within the $[Cu(dmf)_6]^{2+}$ (203(3) pm).[27]

Both $[CuCl_3(dmf)]^-$ and $[CuCl_4]^{2-}$ complexes have a distorted tetrahedral structure. The Cu-O bond length (230(13) pm) within the $[CuCl_3(dmf)]^-$ complex is significantly longer than that of the equatorial Cu-O bonds in the $[Cu(dmf)_6]^{2+}$(203(3) pm)[27] and the $[CuCl(dmf)_5]^+$(199(1) pm). The DMF molecule within the trichlorocuprate(II) complex much more weekly solvates the central metal ion than the DMF molecules within the $[Cu(dmf)_6]^{2+}$ and $[CuCl(dmf)_5]^+$ complexes. On the other hand, the Cu-Cl distance of 225(1) pm within the $[CuCl_4]^{2-}$ complex is longer than that (219(1) pm) in $[CuCl_3(dmf)]^-$. The lengthening of the coordination bond with an increase in the number of chloride ions bound to the copper(II) ion may be caused by an increase in the electron donation of the chloride ions coordinated to the central metal ion and in the electrorepulsive force among the ligands.

The work has been financially supported by the Grant-in-Aid for Special Project Research No. 61134043 from the Ministry of Education, Science and Culture. Computer calculations were performed at the computer center of the Institute for Molecular Science in Okazaki.

## References

1) J. R. Bell, J. L. Tyvoll, and D. L. Wertz, *J. Am. Chem. Soc.*, **95**, 1456 (1973).
2) M. Magini, *J. Chem. Phys.*, **74**, 2523 (1981).
3) G. W. Neilson, *J. Phys. C*, **15**, L233 (1982).
4) P. Lagarde, A. Fontaine, D. Raoux, A. Sadoc, and P. Migliardo, *J. Chem. Phys.*, **72**, 3061 (1980).
5) M. Ichihashi, H. Wakita and I. Masuda, *Bull. Chem.*

Table 5. Results of the Least-Squares Calculation for the Structural Parameters of the Distorted Tetrahedral $[CuCl_4]^{2-}$ Ion. The Values in Parentheses Represent Standard Deviations

| Interaction | Parameter | Solution C | Solution D |
|---|---|---|---|
| Cu-Cl | $r$/pm | 226.1(4) | 225.1(2) |
| | $b$/10 pm$^2$ | 5.9(3) | 7.6(5) |
| | $n$ | 4[a] | 4[a] |
| Cl···Cl | $r$/pm | 346(2) | 345(2) |
| | $b$/10 pm$^2$ | 14(1) | 14(3) |
| | $n$ | 4[a] | 4[a] |
| Cl···Cl | $r$/pm | 414(5) | 411(5) |
| | $b$/10 pm$^2$ | 28(10) | 23(7) |
| | $n$ | 2[a] | 2[a] |

a) The values were kept constant during the calculation.

*Soc. Jpn.*, **56**, 3761 (1983).
6) S. C. Abrahams and H. J. Williams, *J. Chem. Phys.*, **39**, 2923 (1963).
7) R. D. Willett, C. Dwiggins, Jr., R. F. Kruh, and R. E. Rundle, *J. Chem. Phys.*, **38**, 2429 (1963).
8) A. W. Schlueter, R. A. Jacobson, and R. E. Rundle, *Inorg. Chem.*, **5**, 277 (1966).
9) R. D. Willett, *J. Chem. Phys.*, **41**, 2243 (1964).
10) J. P. Steadman and R. D. Willett, *Inorg. Chem.*, **4**, 367 (1970).
11) F. Barendregt and H. Schenk, *Physica*, **49**, 465 (1970).
12) G. L. Ferguson and B. Zaslow, *Acta Crystallogr., Sect. B*, **27**, 849 (1971).
13) R. L. Harlow, W. J. Wells, III, G. W. Watt, and S. H. Simonsen, *Inorg. Chem.*, **13**, 2106 (1974).
14) B. Morosin and E. C. Lingafelter, *J. Phys. Chem.*, **65**, 50 (1961).
15) M. Bonamico, G. Dessy, and V. Vaciago, *Theor. Chim. Acta*, **7**, 367 (1967).
16) J. H. Russell and S. C. Wallwork, *Acta Crystallogr., Sect. B*, **25**, 1691 (1969).
17) A. C. Bonamartini, M. Nardelli, C. Palmieri, and C. Pelizzi, *Acta Crystallogr., Sect. B*, **27**, 1775 (1971).
18) Par J. Lamotte-Brasseur, L. Dupont, and O. Dideberg, *Acta Crystallogr., Sect. B*, **29**, 241 (1973).
19) S. Ishiguro, B. G. Jeliazkova, and H. Ohtaki, *Bull. Chem. Soc. Jpn.*, **58**, 1143 (1985).
20) S. Ishiguro, B. G. Jeliazkova, and H. Ohtaki, *Bull. Chem. Soc. Jpn.*, **58**, 1749 (1985).
21) S. Ishiguro, H. Suzuki, B. G. Jeliazkova, and H. Ohtaki, *Bull. Chem. Soc. Jpn.*, **59**, 2407 (1986).
22) M. A. Khan and M. J. Schwing-Weill, *Inorg. Chem.*, **15**, 2202 (1976).
23) H. Ohtaki, *Rev. Inorg. Chem.*, **4**, 103 (1982).
24) G. Johansson and M. Sandström, *Chem. Scr.*, **4**, 195 (1973).
25) T. Yamaguchi, Doctor Thesis, Tokyo Institute of Technology, March (1978).
26) H. Ohtaki, S. Itoh, T. Yamaguchi, S. Ishiguro, and B. M. Rode, *Bull. Chem. Soc. Jpn.*, **56**, 3406 (1983).
27) K. Ozutsumi, S. Ishiguro, and H. Ohtaki, *Bull. Chem. Soc. Jpn.*, in press.
28) H. Ohtaki, T. Yamaguchi and M. Maeda, *Bull. Chem. Soc. Jpn.*, **49**, 701 (1976).
29) H. Ohtaki and H. Wada, *J. Solution Chem.*, **14**, 209 (1985).